

Structure of Microjet Methane Diffusion Flames

T. S. Cheng¹, Y.-H. Li², C.-S. Chen², C.-Y. Wu², C.-P. Chen², and Y.-C. Chao²

¹Department of Mechanical Engineering, Chung Hua University, Hsinchu, Taiwan, 300, ROC

²Institute of Aeronautics and Astronautics, National Cheng Kung University, Tainan, Taiwan, 701, ROC

E-mail: tscheng@chu.edu.tw

Introduction

Laminar jet diffusion flames can be classified into three types: the Burke-Schumann flame [1] controlled by diffusion, the Roper flame [2] controlled by buoyancy, and microflame [3] controlled by diffusion and momentum. The first two types of flames have been extensively investigated [4]. However, the third type of flame was only investigated by Ban et al. [3] and followed by Nakamura et al. [5]. Recently, numerous researches [6-9] have been devoted to understanding the microjet flames, due to their fundamental aspects and engineering applications. Based on past studies, the microjet flame has sufficiently small size (a few millimeters) and exhibits in spherical shape at various orientation angles indicating its buoyancy insensitivity. Because of its spherical flame shape assimilated to a microgravity flame, it is possible to become the model of microgravity flame that is easy to be established in normal gravity. Also, due to the fact that its size is so small, the amount of heat released from the flame is very small, whereas the heat loss to the burner would be extensively large. This indicates that the flame might be always operated in a severe condition. Moreover, the thickness of diffusive transport layer is the same order as that of reaction-enhanced layer [5] due to its small size. This suggests that the detailed structure of convection-diffusion phenomena or diffusion processes in microjet flames is worth to investigate. In addition, the microjet flame can be used as a point heat source with no preference for the orientation angle in future micro power devices. Therefore, it is necessary to determine the smallest stable flames that can be maintained and to investigate the mechanisms responsible for their quenching. This paper presents results of experimental and theoretical studies of flame shape, flame length, and extinction limit of microjet methane diffusion flames.

Experimental and Theoretical Methods

The microjet methane diffusion flames investigated here are stabilized on vertical straight stainless-steel tubes with nominal diameter (d) ranging from 150 to 770 μm . Fuel is introduced through the tube into the quiescent atmospheric air. The flow rates of the fuels are measured with mass flowmeter, which is calibrated using soap-bubble flow meter. The flame shapes are recorded using color CCD camera with macro lens. Flame dimensions are then determined from the recorded images. The spherical shape of the microjet flames at low flowrates strongly suggests that these flames are primarily controlled by convection-diffusion and that buoyancy effects are minor, at least near the quenching limit. It has been shown [10] that simple models that derived from similarity analysis can adequately predict flame height and flame shape for laminar diffusion flames. For a steady, axisymmetric, vertical laminar jet with low Mach number, uniform pressure, negligible buoyancy, and negligible mass diffusion, heat conduction as well as viscous action in the axial direction but fast chemical reaction rates, the governing non-dimensional differential equations are given as follows:

$$u^* \frac{\partial u^*}{\partial x^*} + v^* \frac{\partial u^*}{\partial r^*} = \frac{1}{\text{Re} r^*} \frac{\partial}{\partial r^*} \left(r^* \frac{\partial u^*}{\partial r^*} \right) \quad (1) \quad \text{and} \quad u^* \frac{\partial f}{\partial x^*} + v^* \frac{\partial f}{\partial r^*} = \frac{1}{\text{Pe} r^*} \frac{\partial}{\partial r^*} \left(r^* \frac{\partial f}{\partial r^*} \right) \quad (2)$$

with the non-dimensional variables defined as $u^* = u/u_e$, $v^* = v/u_e$, $x^* = x/d$, $r^* = r/d$, $\text{Re} = u_e d / \nu$, and $\text{Pe} = u_e d / D$. Equation 10 can be further reduced to an ordinary differential equation by using the stream

function and similarity variables [11] as: $\zeta F'' + F'(F-1) = 0$ (3), which satisfies the boundary condition $\zeta = 0: F = 0, F' = 0$. Equation 3, which is derived by assuming negligible axial diffusion in the flame, can be solved numerically using Runge-Kutta method to obtain F and F' . Ban et al. [4] has shown that the flame shapes calculated with the axial diffusion term are in much better agreement with the measured flame shapes for low Re C_2 class hydrocarbon microflames. If the axial diffusion term is taken into account and using the non-dimensional variables, stream function, and similarity variables, then the differential equation becomes $\left(\frac{\zeta^3}{\gamma^2} + \zeta\right)F'' + F'(F-1) = 0$ (4), with the far-field boundary conditions as $\zeta \rightarrow \infty, F = 0$, and $F' = 0$. In the present study, Eqs. 3 (without axial diffusion) and 4 (with axial diffusion) are both solved numerically to obtain the flame shapes. the flame length is at the axial position as $\zeta \rightarrow 0, x_{fl}^* = \frac{\gamma^2}{Re f_{st}} F''(0)$ (5), where x_{fl}^* is the dimensionless flame height, f_{st} is the stoichiometric value (0.054 for CH_4) of the mixture fraction, and $F''(0) = 2$. Comparisons of the measured and theoretical results are made to verify the effect of axial diffusion in microjet diffusion flames.

Results and Discussion

Figure 1 shows some of photographs of diffusion flames stabilized on a 186 μm (i.d) tube. In the photograph, the bright and blue colors indicate greatest and lowest light intensity, respectively. As long as no soot is formed and the flame is blue as shown in Fig. 1 (i.e., the radiation is primarily from chemiluminescence), the light intensity is approximately proportional to reaction rate. Thus, the bright regions are zones of maximum heat release rate. Near the quenching limit ($Q_f = 3.9$ cc/min), the flame appears as a small blue “cap” centered above the tube. As the fuel flowrate is increased, the flame is stretched in the vertical direction, and the “wings” of highest intensity break apart at the tip, producing annular regions of high reaction rate. The appearance of microjet methane flames observed in the present study is very similar to that of propane flames [8].

Equations 3 and 4 are solved numerically to obtain flame shapes. Comparison of the predicted and measured flame shapes for the $d = 186$ μm flame operated at several fuel exit velocities is plotted in Fig. 2. The measured flame shapes are indicated by symbols and solid and dashed lines denote those from the calculation with and without axial diffusion, respectively. Figure 2 indicates that the flame shapes calculated with and without axial diffusion are in poor agreement with the experimental data and the flame heights are also over-predicted for all ranges of fuel flow rates. Figure 2 demonstrates that the simple jet flame theory, which can properly predict the flame shapes of C_2 class hydrocarbon microflames [3] and of propane microflames [8], fail to predict the flame shapes of microjet methane flames.

Comparison of the measured and calculated flame lengths over Reynolds number ranging from quenching to blowoff for flames stabilized on $d = 186$ and 324 μm tubes is shown in Fig. 3. Figure 3 demonstrated that a simple jet flame theory over-predicts the flame height. The measured nondimensional flame length scales well with $0.2Re$.

To investigate the effect of tube size on extinction behavior, different tube diameter is used. Figure 4 shows photographs of flames operated at fuel exit velocity just above extinction for tube diameters varying from 186 to 778 μm . The most notable feature of Fig. 4 is that the standoff distance is essentially the same, about 0.78 mm, for all the tubes. In addition, the flame shapes are remarkably similar over the range of tube diameters. This implies that the jet diffusion flame theory may be used to predict the fuel exit velocity at quenching.

It has been demonstrated that the measured and predicted flame lengths are a function of Reynolds number only. Accordingly, a flame can not be sustained if the fuel exit velocity for which the predicted flame length is smaller than the measured standoff distance. Thus, it is hypothesized that the critical fuel exit velocity at quenching is that at which the predicted flame length equals the measured standoff distance [8]. The quenching velocity for different tube sizes is determined by equating the flame length in Eq. 5 to the measured standoff distance. Comparison of the measured and calculated quenching velocities is depicted in

Fig. 5. The predicted quenching velocities (dashed line) are lower than the measured data; however, with a modification of simple flame model, the calculated results (solid line) are in good agreement with the measured velocities. It is also found that the modified quenching curve follows $Re \times d = \text{const.}$ ($u \times d^2 = c$). This finding is in agreement with the curve proposed by Ida et al. [7] but different from $Re \times d^2 = C$ that proposed by Nakamura et al. [9].

Conclusions

The flame shape, flame length, and quenching limit of microjet methane diffusion flames operated at fuel exit velocity ranging from just above quenching to below blowoff for tube diameters varying from 186 to 778 μm are investigated. Comparisons of the measured flame heights, flame shapes, and quenching velocities with theoretical predictions indicate that a simple jet flame model can not properly predict the characteristics of microjet methane flames. However, with modification of the model, the predictions are in good agreement with the measured data. Comparisons of predicted quenching velocity with measured results indicate that quenching occurs when the flame length equals the standoff distance. It is also found that the quenching curve follows $Re \times d = \text{const.}$

Acknowledgment

This research was supported by the National Science Council of the Republic of China under Grant numbers NSC92-2212-E-216-001.

References

1. Burke, S. P. and Schumann, T. E. W. (1928) Diffusion flames. *Ind. Eng. Chem.*, **20**, 998-1004.
2. Roper, F. G. (1977) The prediction of laminar jet diffusion flame sizes: Part I. Theoretical model and Part II. Experimental verification. *Combust. Flame*, **29**, 219-234.
3. Ban, H., Venkatesh, S. and Saito, K. (1994) Convection-diffusion controlled laminar micro flames. *J. Heat Transfer*, **116**, 954-959.
4. Williams, F. A. (1985) *Combustion Theory*, 2nd Ed., Addison-Wesley, New York.
5. Nakamura, Y., Ban, H., Saito, K. and Takeno, T. (1997) Micro diffusion flames in a cold boundary. *Proc. of the Central State Section Meeting*, 160-163.
6. Nakamura, Y., Ban, H., Saito, K. and Takeno, T. (2000) Structure of micro (millimeter size) diffusion flames. *Proc. of the 3rd International Symposium on Scale Modeling*, Nagoya, Japan.
7. Ida, T., Fuchihata, M. and Mizutani, Y. (2000) Microscopic diffusion structures with micro flames. *Proc. of the 3rd International Symposium on Scale Modeling*, Nagoya, Japan.
8. Matta, L. M., Neumeier, Y., Lemon, B. and Zinn, B. T. (2002) Characteristics of microscale diffusion flames. *Proc. of the Combustion Institute*, **29**, 933-939.
9. Nakamura, Y., Kubota, A., Yamashita, H. and Saito, K. (2003) Near extinction flame structure of micro-diffusion flames. *The International Symposium on Micro-Mechanical Engineering*, Paper No. ISMME2003-111.
10. Spalding, D. B. (1979) *Combustion and Mass Transfer*, 1st Ed., Pergamon Press, New York.
11. Schlichting, H. (1987) *Boundary-Layer Theory*, 7th Ed., McGraw-Hill, New York.

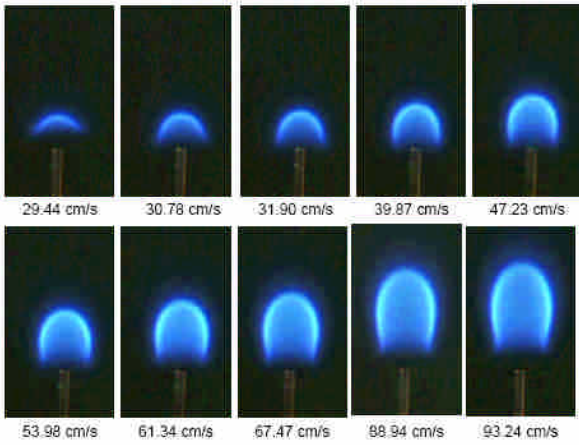


Fig. 1. Photographs of flames supported on a 186 μm tube.

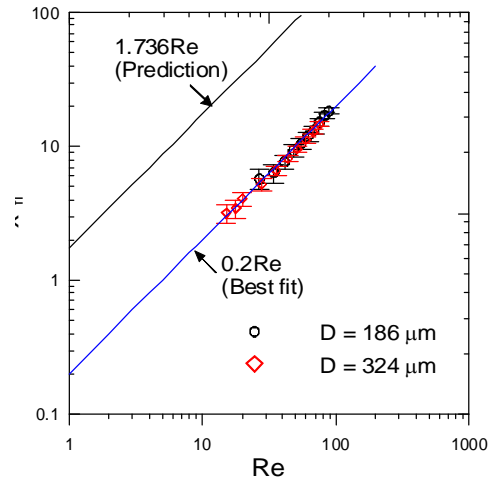


Fig. 3. Comparison of the calculated and measured nondimensional flame lengths as a function of Re for $d = 186$ and $324 \mu\text{m}$ tubes.

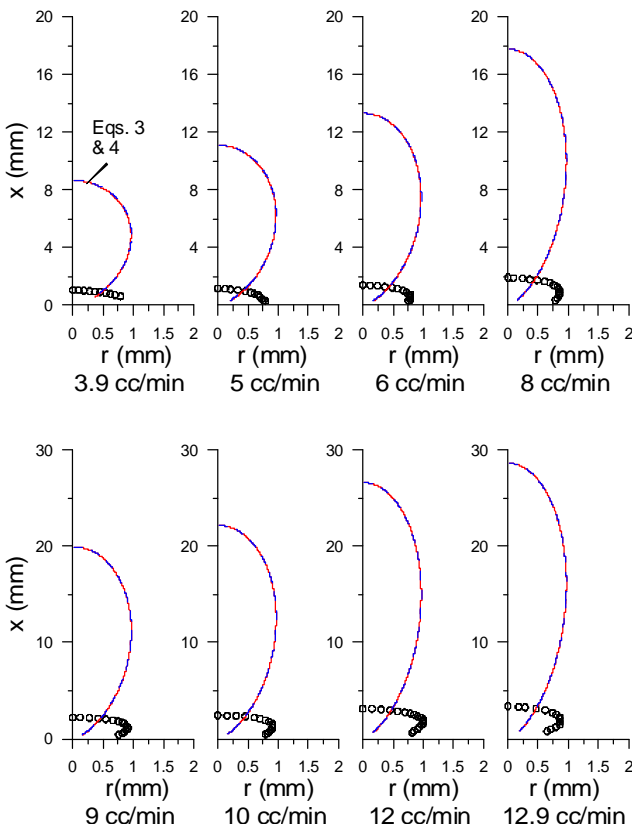


Fig. 2. Comparison of the calculated and measured flame shapes for $d = 186 \mu\text{m}$ tube.

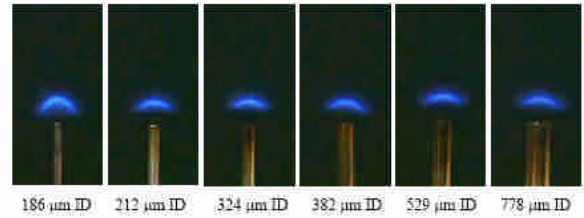


Fig. 4. Photographs of flames just above quenching limit for different tube diameters.

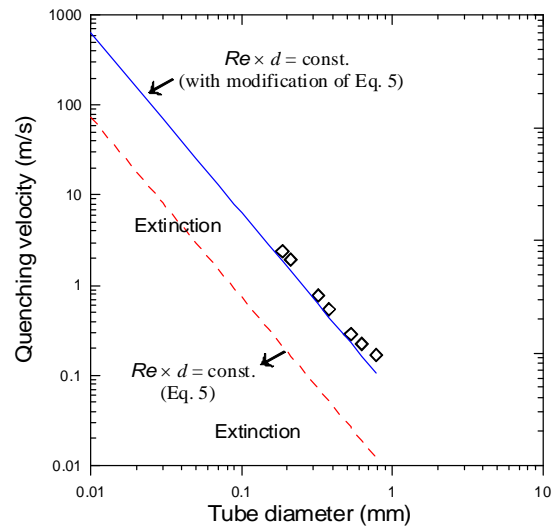


Fig. 5. Comparison of the predicted and measured quenching velocities as a function tube diameter.